

The vaporisation of liquid injected into a fracture bounded by impermeable superheated rock

Andrew W. Woods,

Centre for Environmental and Geophysical Flows,
School of Mathematics, University of Bristol, Bristol,
England, BS8 1TW: a.w.woods@bris.ac.uk

Shaun D. Fitzgerald, Catherine Wang

Stanford Geothermal Program, Stanford University

January 1998

We describe a theoretical model of the fluid flow, heat transfer and phase change which occurs when liquid is injected into a fracture bounded by a hot, impermeable rock. We first consider the case of a warm host rock, in which there is no boiling of the water. We then develop the model to describe the case in which the host rock temperature is in excess of the boiling temperature and the water boils. We show that a two-phase boiling zone develops between purely liquid and purely vapour filled regions in the fracture. The results are compared successfully with new laboratory experiments in which both water and ether spread radially from a central source into a fracture consisting of two hot glass plates. The work has direct implications for understanding vapour regeneration as a result of liquid injection and boiling in a geothermal reservoir.

1. Introduction

In many superheated geothermal reservoirs, vapour is drawn from the system to generate power. In an attempt to regenerate this vapour, commercial operators actively reinject liquid. The fate of this liquid depends on the properties of the reservoir, and in particular, whether the system is dominated by large fractures or may be represented as a porous matrix. A number of recent models and laboratory experiments have analyzed the injection, propagation and ultimately the boiling of liquid in a superheated porous layer (Pruess et al., 1987; Woods and Fitzgerald, 1993; Woods and Fitzgerald, 1997). These studies have identified some of the fundamental controls on the heat transfer and phase change in hot permeable rock. However, the models only apply to flow in a porous layer, while in many geothermal systems, the liquid motion may be dominated by flow along large fractures. Here we report on the results of a complementary study in which we examine the heating and phase change which occurs when liquid is injected into a fracture embedded between two impermeable layers of rock.

We consider two-dimensional flow, discussing the physical balances which control the process. Then we present some simple analytical solutions which are valid

in the limit of small and large Stefan number. We extend the analysis to describe the axisymmetric spreading from a point source, for which a different class of similarity solutions are required. The predictions of the axisymmetric model are then compared with a series of laboratory experiments in which liquid was injected into a fracture surrounded by impermeable boundaries at a temperature (i) below the boiling point, and (ii) above the boiling point. We conclude with a discussion of the relevance of the work for modelling injection into geothermal systems.

2. Physical balances controlling heat transfer and boiling in a fracture

When liquid invades a fracture in one-dimension as shown in figure 1, heat is transferred from the surrounding walls by thermal conduction. After a time t , the conduction will have cooled the walls a distance of order $(\kappa t)^{1/2}$ in the direction normal to the fracture and a distance $x(t)$ along the fracture. $x(t)$ may be calculated in terms of the global conservation of heat.

2.1 Host rock below the vaporisation temperature.

If the volume of liquid injected after time t (per unit length in the cross-flow direction) is Qt and the initial temperature of the liquid is ΔT cooler than the host rock, then the heat required to raise the temperature of the injected liquid to that of the rock, $\rho_l C_{pl} \Delta T Qt$, is supplied by cooling the volume (per unit length in the cross-flow direction) of rock $\sim \rho_r C_{pr} \Delta T (\kappa t)^{1/2} x(t)$. Therefore, we expect that

$$x(t) \sim R_l P \kappa^{1/2} t^{1/2} \quad (2.1)$$

where

$$R_l = \frac{\rho_l C_{pl}}{\rho_r C_{pr}} \quad \text{and} \quad P = Q/\kappa \quad (2.2, 2.3)$$

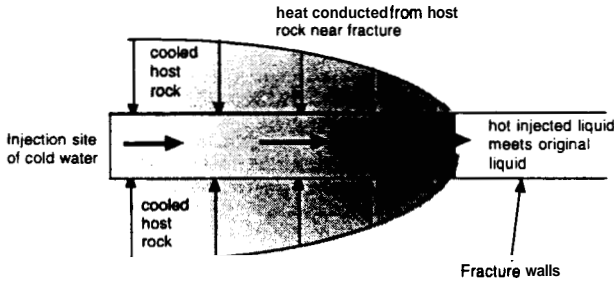
For a constant injection rate, these scalings show that the cooled region extends a distance

$$x(t) \sim R_l P (\kappa t)^{1/2} \quad (2.4)$$

2.2 Host rock above the boiling temperature. If the fracture walls are initially above the boiling temperature of the liquid, then three separate zones develop in the fracture. Near the site of injection, the liquid is heated from the injection temperature to the boiling temperature. Ahead of this region, the thermal energy is used to vaporise the liquid producing an isothermal two-phase boiling zone of length $y(t)$ say along the fracture. The temporal dependence of $y(t)$ may be found from a simple heat balance

$$\rho_r C_{pr} \Delta T_b y(t) (\kappa t)^{1/2} \sim \rho_l L Q t \quad (2.5)$$

Figure 1



1. Schematic of heat transfer into a fracture from the host rock

where L is the heat of vaporisation, and ΔT_b is the temperature of the fracture walls in excess of the boiling temperature. This leads to the scaling for the thickness of the boiling zone

$$y(t) \sim R_1 S P (\kappa t)^{1/2} \quad (2.6)$$

where

$$S = L / C_{pl} \Delta T_b \quad (2.7)$$

is the Stefan number of vaporisation. Finally, ahead of the two-phase zone, the newly formed vapour is heated up to the far-field temperature over a distance $z(t)$, where, as in (2.2),

$$z(t) \sim R_v P (\kappa t)^{1/2} \quad (2.8)$$

with $R_v = \frac{\rho_v C_{pv}}{\rho_r C_{pr}}$, the ratio of specific heats of the vapour and host rock.

These scalings are appropriate as long as the cross-fracture conduction of heat through the fracture walls dominates the along fracture conduction of heat, so that there is negligible cooling of the walls ahead of either the boiling zone or the zone in which the liquid or vapour is being heated. The cross-fracture conduction of heat only dominates the along-fracture conduction if

$$P, SP \gg 1 \quad (2.9)$$

In many situations of interest, (2.9) is satisfied and hence the scalings (2.4, 2.6, 2.8) provide simple estimates for the length of the zone over which liquid or vapour is heated or the length of the boiling zone.

3. A model of heating and boiling in a fracture

Complete solutions, which provide the dimensionless constants for the scalings presented above may be found by complete solution of the governing equations. This shows that, for the case of no boiling, the temperature in the host rock is given by

$$T(x, y, t) = T_i + \Delta T \operatorname{erf} \left(\frac{y + \frac{x}{R_1 P}}{(\kappa(t - wx/Q))^{1/2}} \right) \quad \text{for } x < Qt/w \quad (3.1)$$

$$T(x, y, t) = T_i + AT \quad \text{for } x > Qt/w \quad (3.2)$$

where the fracture width is w (figure 2).

When the initial temperature of the host rock is in excess of the boiling temperature, the process becomes more complex. However, in the limiting case that (i) the heat of vaporisation is much greater than that required to heat the liquid to the boiling temperature or to heat the vapour to the far-field temperature once it has boiled, $L \gg C_p \Delta T_1, C_p \Delta T_2$, and (ii) $QS/\kappa \gg 1$ so that heat conduction in the along-fracture direction may be neglected relative to that in the along fracture direction, there is a much simplified solution of the system. In this limit, the boiling zone dominates and therefore the temperature profile may be approximated by

$$T = T_b + \Delta T \operatorname{erf} \left(\frac{y}{(\kappa t - x^2/\lambda^2)^{1/2}} \right) \quad \text{for } 0 < x < \lambda(\kappa t)^{1/2} \quad (3.3)$$

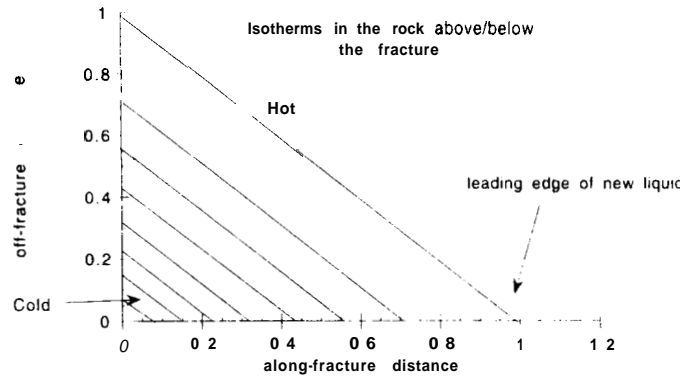
and $T = T_b + AT$ for $x > \lambda(\kappa t)^{1/2}$ where $\lambda = \frac{2QS R_1}{\pi \kappa}$ with the leading edge of the boiling zone located at

$$L_2(t) = \lambda(\kappa t)^{1/2} \quad (3.4)$$

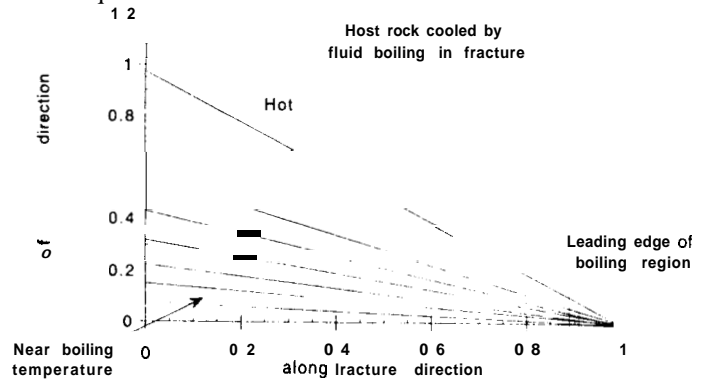
Further, the mass flux of vapour as a function of the total mass flux in the fracture varies with position according to (figure 4)

$$\phi(x, t) = \frac{2}{\pi} \sin^{-1} \left(\frac{x}{\lambda(\kappa t)^{1/2}} \right) \quad \text{for } 0 < x < \lambda(\kappa t)^{1/2} \quad (3.5)$$

In this approximate solution, shown in figure 3, the relatively narrow regions in which liquid is heated to the boiling temperature and in which vapour is heated to the far-field temperature are neglected.



2. Solution of the temperature profile in the host rock as liquid invades the rock and heats it up



3. Temperature profile in the host rock when there is a zone of boiling.

4. Axisymmetric Injection

The problem of axisymmetric injection into a fracture is also of interest, but requires new scaling laws for the distances over which liquid is heated up and boils. Applying similar arguments for the conservation of heat to those of section 2, we find that the radial distance over which liquid is heated from one temperature to a second scales as

$$r(t) \sim \left(\frac{RQ}{\pi\kappa^{1/2}} t^{1/2} \right)^{1/2} \quad (4.1)$$

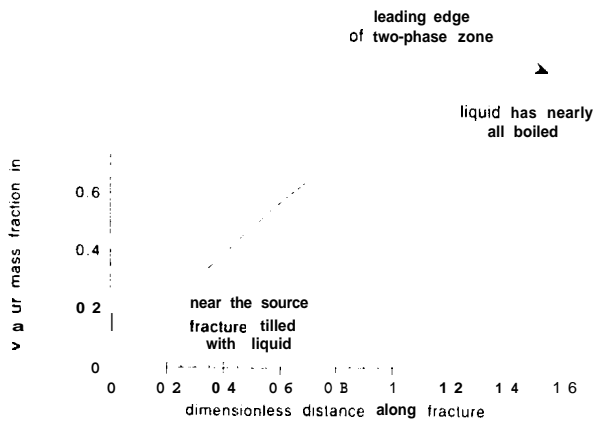
while the radial distance over which liquid boils scales as

$$r(t) \sim \left(\frac{RQS}{\pi\kappa^{1/2}} t^{1/2} \right)^{1/2} \quad (4.2)$$

These solutions only apply as long as the radial conduction scale is much smaller than the radial location of the front, so that a negligible amount of heat is conducted inwards from larger radii. The scalings only apply for times

$$t \ll \tau = (RSQ^2/\pi\kappa^{3/2})^2 \quad (4.3)$$

For typical values in geothermal systems, $R_1 \sim 1$, $Q \sim 10^{-5} - 10^{-1} \text{ m}^3/\text{s}$, $\kappa \sim 10^{-6} \text{ m}^2/\text{s}$, and $S \sim 10 - 100$, so that, this scaling applies at least for times $0 < t \ll 10^9 \text{ s}$, which covers the time of interest for geothermal systems, which is typically of order months to years. Therefore we may neglect the effects of radial conduction of heat in applying the model to actual reservoirs.



4

4.2 Asymptotic solution for boiling in a radial fracture

As in section 3, there is a useful asymptotic solution for the temperature profile in the limit of high Stefan number, $S = L/C_p \Delta T \gg 1$, in which case the heat of vaporisation is much larger than the heat required to warm up the injected liquid or heat the newly formed vapour. In this approximation, $r_1 \ll r_2$, and the length of the zone ahead of the boiling region in which the vapour is heated to the far-field temperature also becomes vanishingly small relative to the boiling zone. The temperature profile therefore has the approximate form

$$T = T_b + \Delta T \text{erf} \left(\frac{y}{(\kappa t - r^4/\lambda^4)^{1/2}} \right) \quad \text{for } r < r_2 = \lambda(\kappa t)^{1/4} \quad (4.4)$$

with

$$\lambda = \left(\frac{2QS}{\kappa\pi^2} \right)^{1/2} \quad (4.5)$$

and the vapour mass flux, as a fraction of the total mass flux, increases with radius according to

$$\phi = \frac{2}{\pi} \sin^{-1} \left(r^2/\lambda^2(\kappa t)^{1/2} \right) \quad (4.6)$$

with the leading edge of the boiling zone located at

$$r = r_2 = \lambda(\kappa t)^{1/4} \quad (4.7)$$

5. Experimental results on boiling in a fracture

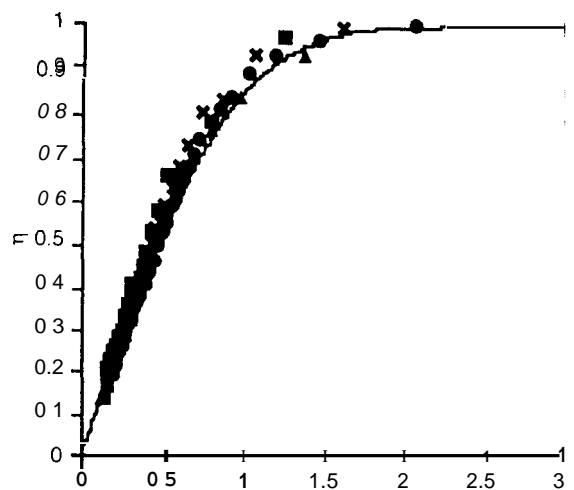
A series of experiments have tested the above scalings for heat transfer and boiling in a fracture

5.1 Fracture walls below the vaporisation temperature

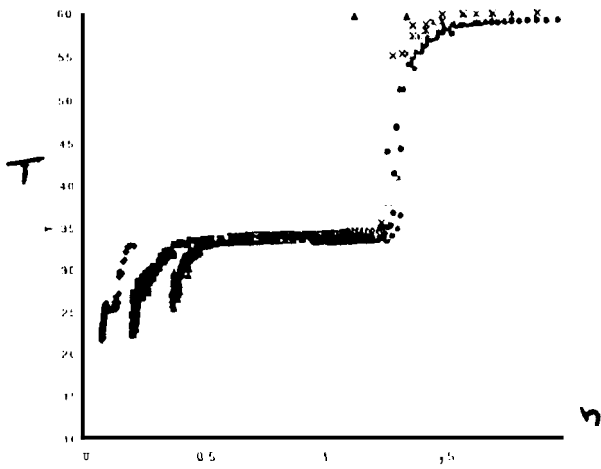
In the first set of experiments, water was injected at a temperature of 20°C and the glass plate was heated to a range of temperatures $40-90^\circ\text{C}$. The dimensionless temperature profile for different experiments with injection rates 3, 6 and 10 ml/min have been plotted on figure 4 as a function of the similarity variable $\eta = r/(Q\kappa t)^{1/4}$. All the experimental data collapses to a single curve, confirming the scaling analysis of section 4.1 (figure 5). Second, there is excellent agreement between the experiments and the model temperature profile (4.10) for the time interval $0 < t < 900 \text{ s}$, corresponding to the data. The analytical solution applies for $1 - 10 \text{ s} = t_u < t < t_c = (Q^2/\kappa^3) = 10^4 \text{ s}$ for the injection rates $Q = 0.5, 1, 1.5 \times 10^{-7} \text{ m}^3/\text{s}$, used in these experiments. We conclude that the new model provides an excellent description of heat transfer as liquid invades a fracture.

5.2 Boiling in a fracture

In the second set of experiments the glass plates were heated to a temperature $T_b + \Delta T_i \sim 60^\circ$. Chile the ether was injected at a temperature of 21° . Again,



5 Comparison of experimental measurements and theoretical predictions for the temperature profile in the fracture as a function of the distance from the source for the case of liquid being heated in the fracture



6. Comparison of the experimental measurements and theoretical predictions of the temperature profile in the fracture as a function of the distance from the source for the case in which liquid ether boils.

various radii from the source, by a series of thermocouples. These thermocouples were arranged at different azimuthal positions in the fracture, rather than along a single radius. In each experiment, red dye was added to the ether. This did not vaporise, and a ring of dye therefore collected at the leading edge of the boiling front as it advanced through the experimental fracture so the position of the leading edge of the boiling front could be determined as a function of time. The boiling zone migrates outwards in an approximately circular fashion.

At atmospheric pressure, the boiling point of the ether is 34° , the specific heat of the ether is approximately $2000 \text{ J kg}^{-1} \text{ K}^{-1}$, and the heat of vaporisation is $3.78 \times 10^5 \text{ J kg}^{-1}$. Therefore, we estimate that the Stefan number

$$S = L/C_p \Delta T_1 \sim 7 \quad (5.1)$$

This is sufficiently large that we might expect the approximate model of the boiling for $S \gg 1$ (section 3) to apply to leading order. In figure 6, the measured temperatures, $(T(\eta) - T_b)/\Delta T_1$, of the thermocouples have been plotted as functions of the similarity variable $\eta = r/(S^2 Q^2/\kappa)^{1/4}$. It is seen that all the temperature profiles collapse to a single curve, corroborating the scaling arguments of section 2 and the model of section 3.

Again, the very good agreement, between the experimental measurements and the theoretical predictions is expected over the time scale of the experiments. In particular, in section 2, we identified that the model predictions should be valid for $t \ll (SQ)^2/\kappa^3 \sim 10^5 \text{ s}$ yet the experiments only run for $t < 900 \text{ s}$.

6. Discussion and Applications

The results suggest that, as liquid migrates along superheated fractures, it is natural that a two-phase zone develops between the liquid region near source and the superheated vapour zone in the far-field (figure 1). For a radially spreading injected fluid, this two-phase zone has length

$$L(t) \sim Q^{1/2} t^{1/4} \kappa^{-1/4} \quad (6.1)$$

For an injection rates into a geothermal reservoir along a wellbore in the range $Q \sim 10^{-4} - 10^{-1} \text{ m}^2/\text{s}$, the scaling (6.1) implies that the two phase zone will extend a distance of order $0.1 - 10 t^{1/4}$ from a point source in a fracture. Thus after times of order 1 year, the two phase zone will extend 10-1000 m from the source. This constrains the possible impact of re-injected liquid on the reservoir pressure, since, in a superheated system, the liquid and two-phase zone remains rather localised about the site of injection.

These results provide new understanding for constraining the number, duration and positioning of reinjection wells which are required in order to maintain an approximately uniform reservoir pressure.

Acknowledgements. This work is supported by Unocal, PGE and the NERC. AWW was also supported by a Blaustein Visiting Professorship at Stanford University during the early stages of this work.

References.

- Ames, W., Numerical methods for partial differential equations, Springer, 1981.
 Barker, BJ, Koenig, BA, Stark, MA, 1995, Water injection management for resource maximisation: observations from 25 years at the Geysers, California, Proc. World Geoth Congress, 3, 1959-1964.
 Fitzgerald, S.D., Pruess, K., van Rappard, D.M., 1996, Laboratory studies of injection into horizontal fractures, Proc. Stanford Geoth. Workshop, 113-118.
 Fitzgerald, S.D., Woods, A.W., Wang, C.T.L., 1997, Injection into geothermal systems, Proc. Stanford Geoth. Workshop, 355-360.
 Pruess, K., Calore, C, Celati, R and Wu, Y.S., 1987, An analytical solution for heat transfer at a boiling front moving through a porous medium, Int J. Heat Mass Trans, 30, 2595-2602
 Woods AW and Fitzgerald, SD, 1993, The vaporisation of a liquid front moving through a hot porous rock, J Fluid Mech., 251, 563-579
 Woods, A.W. and Fitzgerald, SD, 1997, The vaporisation of a liquid front moving through a hot porous rock. Part 2. Slow injection, J Fluid Mech., 343, 303-316